

---

# Model Fusion via Neuron Interpolation

---

Phoomraphee Luenam<sup>\*1</sup>

Andreas Spanopoulos<sup>\*1</sup>

Amit Sant<sup>\*1</sup>

Thomas Hofmann<sup>1</sup>

Sotiris Anagnostidis<sup>1</sup>

Sidak Pal Singh<sup>1</sup>

<sup>1</sup>ETH Zürich, Switzerland

## Abstract

Model fusion aims to combine the knowledge of multiple models by creating one representative model that captures the strengths of all of its parents. However, this process is non-trivial due to differences in internal representations, which can stem from permutation invariance, random initialization, or differently distributed training data. We present a novel, neuron-centric family of model fusion algorithms designed to integrate multiple trained neural networks into a single network effectively regardless of training data distribution. Our algorithms group intermediate neurons of parent models to create target representations that the fused model approximates with its corresponding sub-network. Unlike prior approaches, our approach incorporates neuron attribution scores into the fusion process. Furthermore, our algorithms can generalize to arbitrary layer types. Experimental results on various benchmark datasets demonstrate that our algorithms consistently outperform previous fusion techniques, particularly in zero-shot and non-IID fusion scenarios. The code is available at: <https://github.com/AndrewSpano/neuron-interpolation-model-fusion>.

## 1 Introduction

As Deep Neural Networks (DNNs) grow larger and larger in scale, the field faces a host of new challenges to deliver good outcomes. Models now are more complex than ever before, often having a unique profile of strengths and weaknesses and requiring increasingly larger datasets and parameters to meet ever increasing performance benchmarks [Sevilla et al., 2022]. This makes the prospect of retraining models on new data from scratch almost certainly expensive and possibly even impossible, such as in cases where data security is paramount. Fusing model parameters addresses both of these issues by not requiring expensive retraining or transmission of sensitive data.

While *ensembling* still provides unparalleled performance, the requirement to maintain many models is becoming increasingly impractical with today’s models. In response to this, recent methods like OTFusion [Singh and Jaggi, 2020], Git Re-Basin [Ainsworth et al., 2022], and a host of federated learning algorithms [McMahan et al., 2017, Wang et al., 2020] have made strides in merging many models into one.

However, with increasingly data-hungry models, training data is often scraped together from a diverse set of sources [Xu et al., 2024, Gao et al., 2020]. Thus, in the fusion context, if avoiding expensive retraining is desired, there is a need for an algorithm that can effectively combine the strengths of models trained with differently distributed training data.

**Contributions.** In this work, we introduce a new family of neuron-centric model fusion algorithms with the following key innovations:

---

<sup>\*</sup>Equal contribution. Correspondence to {luenamp, aspanopoulos, amsant}@ethz.ch

- **Principled formulation of fusion as a representation matching problem.** We provide a formal perspective on neuron-level fusion by decomposing the fusion objective into two interpretable components: grouping and approximation. This formulation leads to a natural and efficient two-stage procedure that enables consistent fusion of models with differing internal representations, including those trained on Non-IID data.
- **Incorporation of neuron importance into the fusion process.** Unlike prior approaches that treat all neurons equally, our methods leverage neuron attribution scores to guide the fusion process toward preserving salient features. We demonstrate that incorporating these scores significantly improves performance – not only in our own methods, but also when retrofitted into existing techniques such as Git Re-Basin. Comparatively, our proposed framework does allow for more flexible alignments and incorporates neuron saliency metrics.

## 2 Related Work

### 2.1 Fusion Algorithms

**OTFusion** [Singh and Jaggi, 2020] formulates neuron alignment as a discrete optimal transport (OT) problem. Given multiple models, OTFusion selects an initial reference model, aligns each of the others’ layers to its layers via optimal transport on neuron activations, and averages the aligned parameters to produce a fused model. One downside of OTFusion is that it was initially designed to handle only linear layers, and hence it could not be applied to arbitrary architectures. Despite this, later work adapted OTFusion to the transformer [Vaswani et al., 2017] architecture [Imfeld et al., 2023]. Our proposed algorithm is more general, as it works on any differentiable DNN architecture, without requiring adaptation as OTFusion does for transformers.

**Git Re-Basin** [Ainsworth et al., 2022] proposes three strategies to perform neuron alignment. In this work, we focus exclusively on the “Matching Activations” approach, which is most directly comparable to our methods that make use of activations. Activation-based Git Re-Basin finds a permutation matrix that minimizes the L2 distance between neuron activations across models. This makes it equivalent to OTFusion, when the latter is made to use an activations-based ground metric. While effective, activations-based Git Re-Basin is limited to pairwise fusion, restricts itself to a one-to-one matching paradigm, and does not account for neuron saliency. We discuss our extension to incorporate scores in Appendix C.

**Federated Learning algorithms.** In federated learning (FL), decentralized clients train local models on private data and periodically send updates to a central server, which aggregates them into a global model. Thus, model fusion on non-IID data distributions is central to FL.

Some of the most well-known methods in this domain include **Federated Averaging (FedAvg)** [McMahan et al., 2017] and **Federated Matching Averaging (FedMA)** [Wang et al., 2020]. The former averages model weights across clients proportionally to the number of local updates or data samples. While simple and popular, FedAvg performs poorly under strong non-IID conditions, as model weights can diverge significantly in the presence of heterogeneous data, especially for deeper Neural Network architectures. FedMA aims to address this challenge by aligning neurons before averaging. However, FedMA requires retraining the fused model after the alignment of every layer to ensure performance recovery, which makes it a *non-zero-shot* fusion algorithm.

Lastly, we briefly mention the traditional methods of aggregating knowledge from different models. **Ensembles**, which average the predictions of base models, typically, represent an upper bound on the performance we can achieve by zero-shot fusion. **Vanilla Averaging** blindly averages the weights of two identical models without alignment. In **Knowledge Distillation (KD)** [Hinton et al., 2015], a model is trained to predict soft-targets originating from other model(s). KD can be applied for any arbitrary group of models, and Li et al. [2024] recently showed it to be quite efficient for vision transformers [Dosovitskiy et al., 2020].

### 2.2 Neuron Attribution

A novel feature of our work is incorporating the optional use of neuron attribution scores, commonly referred to as *neuron importance scores*, into the fusion process to bias the preservation of salient features. **Uniform** importance distributes an equal weight of  $1/n$  on each neuron in a layer of

$n$  neurons. **Conductance** [Dhamdhare et al., 2018] extends *Integrated Gradients* [Sundararajan et al., 2017], which attributes feature importance by integrating gradients along a straight-line path from a baseline input to the actual input. Conductance applies the chain rule to propagate these importance scores to hidden neurons, enabling internal saliency estimation. **DeepLIFT** [Shrikumar et al., 2017] provides another method for attributing importance scores to neurons. It computes the contribution of each neuron by comparing its activation to a reference activation and propagating these differences through a modified chain rule. Unlike gradient-based methods, DeepLIFT can assign non-zero importance scores even when gradients are zero or poorly behaved and requires only a single backward pass, making it computationally efficient.

### 3 Motivation

In a neural network, each group of neurons within a hidden state can be interpreted as encoding a specific amount of information which is used by future layers to produce an output. Consequently, minimizing information loss during fusion is crucial to model performance. We can approximate the information held by a neuron by looking at its distribution across a variety of inputs. Empirically, in adjacent tasks like model pruning, it has been shown that removing neurons with high correlation to other neurons to minimize information loss is effective [Ebid et al., 2025]. We employ the squared Euclidean distance as a proxy for information loss due to its greater computational efficiency and because it has been shown that minimizing the Euclidean distance between normalized vectors is equivalent to maximizing the Pearson Correlation [Berthold and Höppner, 2016]. By weighing this loss with importance scores, we especially penalize distorting more essential neurons. This motivates a method that explicitly minimizes this *neuron distance* between the fused neuron and its predecessors from the base models on average. Alternatively, one can conceptualize the objective as placing the activations of the fused model at any layer “close” to all the activations of the base models at that same layer. We now introduce the necessary notation to formalize this approach.

A (Deep) Neural Network (DNN) is a function  $f_{\mathbf{w}} : \mathbb{R}^d \mapsto \mathbb{R}^o$  parameterized by weights  $\mathbf{w}$  where  $d$  is the number of input features and  $o$  is the number of output features. DNNs can be conceptualized as a “composition” of  $L$  sequential functions:  $f_{\mathbf{w}} = f_{\mathbf{w}_L}^L \circ \dots \circ f_{\mathbf{w}_1}^1$ . Additionally, we can *arbitrarily* group those functions into so-called **composition-levels**. For example, we can decompose  $f_{\mathbf{w}} = f_{\mathbf{w}_3}^3 \circ f_{\mathbf{w}_2}^2 \circ f_{\mathbf{w}_1}^1$  into  $f_{\mathbf{w}} = \widehat{f}_{\widehat{\mathbf{w}}_2}^2 \circ \widehat{f}_{\widehat{\mathbf{w}}_1}^1$ , where  $\widehat{f}_{\widehat{\mathbf{w}}_2}^2 = f_{\mathbf{w}_3}^3$  and  $\widehat{f}_{\widehat{\mathbf{w}}_1}^1 = f_{\mathbf{w}_2}^2 \circ f_{\mathbf{w}_1}^1$ . Functionally, levels are simply a paradigm through which one can flexibly partition a DNN into a favorable composition of functions. An observation worth mentioning is that layers with branching (e.g. skip connections) can be contained in one level to satisfy the sequential compositionality. Given that function composition is associative, we gain the flexibility of partitioning DNNs of different width/depths into networks with the *same number of levels*.

We now introduce notation regarding fusion. Let  $\{M_1, M_2, \dots, M_n\}$  be a collection of pretrained base models. Each model is strategically partitioned to have  $L$  levels. For a given input  $\mathbf{x} \in \mathbb{R}^d$ , let  $\mathbf{z}^{M_k, i}(\mathbf{x}) \in \mathbb{R}^{d^{M_k, i}}$  be the output vector at level  $i$  of model  $M_k$ . Note that the output  $\mathbf{z}$  is a function of the weights  $\mathbf{w}^{M_k, i}$  the input  $\mathbf{x}$  and previous levels – but we omit them to simplify notation. For convolutional and transformer outputs, we define as  $d^{M_k, i}$  the output channels and hidden size, respectively, and the remaining dimensions can be flattened out with the batch dimension.

We denote by  $\mathbf{z}^i = \text{concat}(\mathbf{z}^{M_1, i}, \dots, \mathbf{z}^{M_n, i}) \in \mathbb{R}^{d^i}$  the concatenated outputs at level  $i$ , of total size  $d^i$ . For a fused model  $\mathcal{F}$ , we write  $\mathbf{z}^{\mathcal{F}, i} \in \mathbb{R}^{l^{\mathcal{F}, i}}$  for its outputs at level  $i$ . We also use  $s_j^i$  for the importance score of neuron  $j$  at level  $i$  (of the concatenated outputs  $\mathbf{z}^i$ ). Now, we can introduce the **representation cost** of using weights  $\mathbf{w}^{\mathcal{F}, i}$  at level  $i$  of the fused model  $\mathcal{F}$  (for a given input  $\mathbf{x}$ ):

$$J_{\mathbf{w}^{\mathcal{F}, i}}(\mathbf{x}) = \sum_{j=1}^{d^i} \min_{k \in \{1, \dots, l^{\mathcal{F}, i}\}} \left\{ \left( z_k^{\mathcal{F}, i}(\mathbf{x}) - z_j^i(\mathbf{x}) \right)^2 \right\} = \min_{\mathbf{P} \in \mathcal{P}} \left\| \mathbf{P} \mathbf{z}^{\mathcal{F}, i}(\mathbf{x}) - \mathbf{z}^i(\mathbf{x}) \right\|_2^2 \quad (1)$$

where  $l^{\mathcal{F}, i}$  is the width of  $\mathcal{F}$  at level  $i$  and  $\mathcal{P}$  is the set of binary right stochastic matrices of dimension  $d^i \times l^{\mathcal{F}, i}$ . Intuitively, for each neuron in the concatenated base outputs  $\mathbf{z}^i(\mathbf{x})$ , we compute the squared L2 distance to **its closest neuron in the fused model output**  $\mathbf{z}^{\mathcal{F}, i}(\mathbf{x})$ , and sum these distances.

To solve for the desired weights  $\mathbf{w}^{\mathcal{F},i}$  of the fused model  $\mathcal{F}$  at level  $i$ , we can minimize this cost:

$$\mathbf{w}^{\mathcal{F},i*} = \arg \min_{\mathbf{w}^{\mathcal{F},i}} \mathbb{E}_{\mathbf{x} \sim D} [J_{\mathbf{w}^{\mathcal{F},i}}(\mathbf{x})] \quad (2)$$

Popular layer-wise fusion algorithms [Singh and Jaggi, 2020, Ainsworth et al., 2022] attempt to solve Eq. (2) by solving for soft/hard permutation matrices, and then proceed to average the aligned weights (of the base models), layer-by-layer. In Section 5 we empirically demonstrate that these algorithms: **a)** fail to perform on par with base models in zero-shot fusion, i.e. they require a fine-tuning phase; and **b)** fail to achieve meaningful transfer knowledge in the non-IID regime.

We hypothesize that these shortcomings arise because: **a)** current algorithms ignore how the fused model evolves across levels, treating each level in isolation by only tracking past permutation or alignment matrices, without accounting for potential non-linear changes in the semantic content of previous level outputs; and **b)** not all neurons contribute equally to a model’s prediction on average, but are getting averaged with equal importance. This can especially be an issue in the non-IID setting, where the activations on unseen data may be noisy or irrelevant.

## 4 Proposed Method

### 4.1 Two-Step Objective

To overcome these limitations we propose two novel ideas. First, we incorporate neuron importance scores in the main objective. This creates the **neuron-aware representation cost** objective:

$$J_{\mathbf{w}^{\mathcal{F},i}}^{\text{IMP}}(\mathbf{x}) = \sum_{j=1}^{d^i} s_j^i \min_{k \in \{1 \dots l^{\mathcal{F},i}\}} \left\{ \left( z_k^{\mathcal{F},i}(\mathbf{x}) - z_j^i(\mathbf{x}) \right)^2 \right\} = \min_{\mathbf{P} \in \mathcal{P}} \left\| \mathbf{S}^i (\mathbf{P} \mathbf{z}^{\mathcal{F},i}(\mathbf{x}) - \mathbf{z}^i(\mathbf{x})) \right\|_2^2 \quad (3)$$

where  $\mathbf{S}^i = \text{diag}(s_1^i, \dots, s_{d^i}^i)^{\frac{1}{2}}$  is a diagonal matrix containing the square roots of neuron importance scores. The key difference from Eq. (1) is the introduction of weights  $s_j^i$ , to account for possibly less important outputs. For notational clarity, we will now omit the input  $\mathbf{x}$ .

Second, we decouple the objective by introducing an auxiliary vector  $\mathbf{T}$  of size  $l^{\mathcal{F},i}$ , which we refer to as the **target vector** and it enables a more tractable decomposition of the cost function. This yields the following Theorem.

**Theorem 1.** *Let  $\mathbf{T} \in \mathbb{R}^{l^{\mathcal{F},i}}$  be a vector whose components are the importance-weighted means of clustered level outputs. Then the cost in Eq. (3) can be decomposed as follows:*

$$J_{\mathbf{w}^{\mathcal{F},i}}^{\text{IMP}} = \underbrace{\sum_{k=1}^{l^{\mathcal{F},i}} \sum_{j:k_j=k} s_j^i \left( z_k^{\mathcal{F},i} - T_k \right)^2}_{\text{approximation error}} + \underbrace{\sum_{k=1}^{l^{\mathcal{F},i}} \sum_{j:k_j=k} s_j^i \left( T_k - z_j^i \right)^2}_{\text{grouping error}} \quad (4)$$

where  $k_j$  are the assignment indices that achieve the minimum in Eq. (3).

*Proof.* See Appendix A. □

We observe that the sum of  $J_{\mathbf{w}^{\mathcal{F},i}}^{\text{IMP}}(\mathbf{x})$  over a batch is subdifferentiable with respect to  $\mathbf{w}^{\mathcal{F},i}$  and that this objective could potentially be optimized with subgradient descent in the same spirit as the weighted K-means objective [Bottou and Bengio, 1994]. However, we leave this for future work.

The resulting objective naturally decomposes into two interpretable components. The **grouping error** measures how well the original neurons cluster together – specifically, how far each output  $z_j^i$  is from the importance-weighted cluster center  $T_k$  it was assigned to. The **approximation error**, on the other hand, quantifies how closely the fused model can reproduce these cluster centers through its own output neurons  $\mathbf{z}^{\mathcal{F},i}$ .

For a batch of  $B$  values of  $\mathbf{x}$ , minimizing the total grouping error by constructing an optimal  $\mathbf{T}$  through an effective clustering of the layer outputs  $z_j^i$  is a critical challenge. This problem corresponds to the K-means problem in  $\mathbb{R}^B$  which is known to be NP-hard in general [Aloise et al., 2009]. Nonetheless,

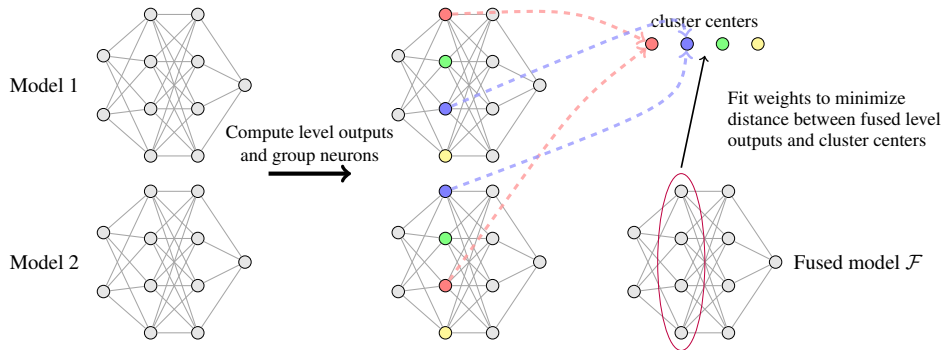


Figure 1: Overview of our method. Given two MLPs with two hidden layers of size 4 with each layer defined as its own level, we compute level outputs for the base models, cluster their neurons, and train the first level of the fused model to match the cluster centers using MSE loss. The process is repeated in subsequent levels.

practical approximation algorithms such as Lloyd’s algorithm [Lloyd, 1982] or local search-based methods [Kanungo et al., 2002] can be employed to obtain effective solutions in practice.

After having determined  $\mathbf{T}$  (and hence, the clusters  $k_j$ ), we can solve for the weights of a level by minimizing the approximation error, which is equivalent to a weighted mean squared error loss function. We can choose to either keep the weights of previous level frozen (and just optimize the current level), or optimize the whole subnetwork. Without loss of generality, we choose the former:

$$\mathbf{w}^{\mathcal{F},i*} = \arg \min_{\mathbf{w}^{\mathcal{F},i}} \mathbb{E}_{\mathbf{x} \sim D} \left[ \sum_{k=1}^{l^{\mathcal{F},i}} \sum_{j:k_j=k} s_j^i \left( z_k^{\mathcal{F},i}(\mathbf{x}) - T_k(\mathbf{x}) \right)^2 \right] \quad (5)$$

This decomposition offers a more interpretable and stable optimization target by isolating the challenges of clustering and function fitting, instead of trying to solve them jointly.

## 4.2 Proposed Algorithm

Following the derivation in Section 4.1, we propose a two-step algorithm to find weights  $\mathbf{w}^{\mathcal{F},i}$  that minimize Eq. (4) in expectation. The algorithm constructs the fused model in a bottom-up way, iterating through the levels of base models, and producing the corresponding level of the fused model.

At each level, the algorithm computes a matching/clustering to minimize the grouping error. It then uses this clustering to compute cluster centers (weighted by importance score). Finally, it uses the cluster centers as a target for the current level’s outputs. We then fit weights of the fused model to minimize the approximation error. In practice, we use a finite batch to approximate the expected representation cost. An intuitive illustration of our algorithm can be found in Fig. 1. High-level pseudo-code is provided in Algorithm 1. For more implementation details, refer to Appendix F.

## 4.3 Minimizing the Grouping and Approximation Errors

### 4.3.1 Grouping Error

For the grouping error, we distinguish between two cases based on the architecture of the base models and the constraints imposed on the assignment. More details can be found in Appendix B.1.

(a) *Equal-size models with level-wise one-to-one matching.* This case induces a cost that can be minimized using the Hungarian Matching algorithm [Kuhn, 1955] as discussed in Section 3. We refer to this special case of our algorithm as **Hungarian Fusion (HF)**.

(b) *General case with arbitrary model sizes.* In this setup, the grouping problem becomes a general clustering task. As highlighted in Section 4.1, a solution can be approximated using heuristic K-means algorithms. We refer to this general case as **K-means Fusion (KF)**.

### 4.3.2 Approximation Error

For the approximation error, we distinguish two cases. More details can be found in Appendix B.2.

---

**Algorithm 1** Neuron Interpolation Model Fusion

---

**Require:** Trained models  $\{M_k\}_{k=1}^n$ , neuron importance scores  $\{s_j^{(i)}\}_{i=1}^L$ , input dataset  $\mathbf{X} \in \mathbb{R}^{B \times d}$

**Ensure:** Fused model  $\mathcal{F}$  with weights  $W_{\mathcal{F}}$

- 1: **for** each level  $i = 1, 2, \dots, L$  **do**
- 2:   Gather layer outputs:  $\mathbf{z}^i = \text{concat}(\mathbf{z}^{M_1,i}, \dots, \mathbf{z}^{M_K,i})$
- 3:   Gather scores:  $\mathbf{s}^i = \text{concat}(\mathbf{s}^{M_1,i}, \dots, \mathbf{s}^{M_K,i})$
- 4:   Obtain an assignment  $k_j$  for every level output  $z_j^i$       {Hungarian Matching or K-means}
- 5:   **for** each centroid  $k = 1, \dots, l^{\mathcal{F},i}$  **do**
- 6:      $T_k^i \leftarrow \frac{\sum_{j:k_j=k} s_j^i z_j^i}{\sum_{j:k_j=k} s_j^i}$       {Compute importance-weighted mean}
- 7:   **end for**
- 8:   Optimize the weights  $\mathbf{w}^{\mathcal{F},i}$  of the current level using:

$$\mathbf{w}^{\mathcal{F},i} \leftarrow \arg \min_{\mathbf{w}} \sum_{m=1}^B \left[ \sum_{k=1}^{l^{\mathcal{F},i}} \sum_{j:k_j=k} s_j^i \left( z_k^{\mathcal{F},i}(\mathbf{x}_m) - T_k^i(\mathbf{x}_m) \right)^2 \right]$$

{Fit Fused Model level output to target means}

9: **end for**

10: **return** Fused Model  $\mathcal{F}$

---

(a) *Linear levels.* When all trainable levels are affine transformations such as fully connected or convolutional layers, the outputs  $z_j^i$  are linear functions of the level weights  $\mathbf{w}^{\mathcal{F},i}$ , and the problem becomes weighted least squares, which has a closed-form solution. In this case, we project the base models' level outputs onto the image of the previous fused level's outputs, before running HF or KF for the level. We call these algorithms the **Linear** version of HF and KF respectively.

(b) *General case.* For arbitrary differentiable (and possibly non-linear) levels, we optimize Eq. (5) using stochastic gradient descent (SGD). In this setting, initialization plays a critical role. A simple strategy is to initialize with the weights of the corresponding level from one of the base models, perturbed by noise  $\epsilon$ . Note that for linear levels, the objective is convex, reducing to case (a). For this case, we will only consider KF and refer to this algorithm as the **Gradient** version of KF.

### 4.3.3 Guarantees

We now present theoretical guarantees for Algorithm 1 under specific conditions.

**Theorem 2.** *Let the parametrized levels of the base models and fused model be affine functions. Then:*

- (a) *For two models with equal-sized levels and a one-to-one matching constraint, the **Hungarian Fusion** algorithm returns an optimal solution to the decoupled objective in Eq. (4).*
- (b) *For an arbitrary number of models with possibly different numbers of neurons per level, the **K-means Fusion** algorithm produces a solution whose representation cost is at most  $(9 + \epsilon)$  times the optimal, when using the local-search algorithm from Kanungo et al. [2002].*

*Proof.* See Appendix A. □

## 5 Experiments

We evaluate our fusion algorithms across three distinct training regimes, each characterized by a different data distribution used to train the base models. This setup is designed to test the robustness and generality of our method. We benchmark our algorithms against previous baselines, ensembles, vanilla averaging, and last-layer knowledge distillation (KD) for non-IID setups. We restrict KD to the last layer because most of the fusion algorithms require only a small amount of data, and applying full KD led to diminished performance due to overfitting in our experiments.

## 5.1 On the Performance of Base Models in Non-IID Setups

Before presenting our results, we emphasize an important consideration in evaluating base model performance under non-IID conditions. In these settings, each model has access to only a small and often imbalanced portion of the dataset, which naturally limits its accuracy. For example, in 6-way or 8-way splits, each model sees only 10-20% of the full data, leading to lower performance compared to centralized training.

Despite these constraints, gains in this setup are meaningful. Improving over weak, heterogeneous base models in a zero-shot setting is a challenging task, and our method demonstrates robustness where baseline methods fail.

## 5.2 Non-IID Setup

The primary goal of our method is to effectively combine the knowledge of similar models trained on unbalanced datasets. To test this, we split the data into unbalanced, non-IID, and disjoint subsets to train each model on. This induces class-specific overfitting and leads to diverse semantic representations, increasing the potential gains from fusion. This setup is also common across Federated Learning applications, where various edge devices have access to a small, skewed subset of the available data. More details about this data partitioning process can be found in Appendix D.

We evaluate algorithms in a *zero-shot* fusion setting, where models are not allowed to retrain after fusing. We train and fuse VGG11s on CIFAR-10 and ViTs on CIFAR-100. In these experiments, all results are averaged over five random seeds used to split the initial datasets and to initialize and train the base models. For each seed, base models are first sorted by performance before being averaged to get the individual performance. Each fusion algorithm is applied once per neuron importance score, and we report the result with the best-performing importance score. Results for VGG11 are shown in Table 1, and for ViT in Table 8.

Table 1: **Test accuracy** comparison when fusing VGG11 networks on CIFAR-10 for **Non-IID** splits. Fusion was performed using 400 data points sampled from the dataset seen by the first model. The same fusion data was used for all algorithms. For the full table, refer to Table 11.

Method	2-WAY SPLIT	4-WAY SPLIT	8-WAY SPLIT
Base Models	81.5, 75.1	77.2, 75.3, 73.6, 66.8	69.2, 68.0, 66.0, 63.0 61.8, 59.6, 56.1, 52.6
Vanilla Averaging	11.2 $\pm$ 2.2	10.0 $\pm$ 0.0	10.0 $\pm$ 0.0
Last-layer KD	82.7 $\pm$ 0.9	60.1 $\pm$ 6.8	43.7 $\pm$ 9.8
Ensemble	87.5 $\pm$ 0.4	83.7 $\pm$ 0.9	76.6 $\pm$ 0.7
OTFusion <sup>1</sup>	43.4 $\pm$ 6.9	20.4 $\pm$ 7.6	12.9 $\pm$ 2.6
Git Re-Basin <sup>1</sup>	71.8 $\pm$ 3.4	N/A	N/A
Hungarian Linear Fusion (Ours)	<b>84.6</b> $\pm$ 0.8	N/A	N/A
K-means Linear Fusion (Ours)	84.5 $\pm$ 0.8	<b>78.9</b> $\pm$ 1.3	<b>69.6</b> $\pm$ 1.2
K-means Gradient Fusion (Ours)	83.3 $\pm$ 1.1	78.6 $\pm$ 2.1	68.6 $\pm$ 4.5

## 5.3 Sharded Setup

The next setup, which we refer to as “sharded”, represents an extreme non-IID case where each model sees all the samples from specific classes, but for a small subset of all classes (per model). Although less common in practice, it serves as a stress test and highlights our method’s robustness.

Similarly to the Non-IID case, we again evaluate our algorithms on *zero-shot* fusion, and for VGGs and ViTs on CIFAR-10 and CIFAR-100 respectively. The experiments setup is the same as with Non-IID. The results for VGGs can be found in Table 9, and the results for ViTs in Table 2.

<sup>1</sup>Git Re-Basin reduces to OTFusion when solving the OT problem exactly with uniform importance scores. In practice, OTFusion uses preactivations [Singh and Jaggi, 2020], while Git Re-Basin uses activations [Ainsworth et al., 2022]; we follow these defaults. Empirically, both yield the same fused model when using preactivations.

Table 2: **Test accuracy** comparison when fusing ViT networks on CIFAR-100 for **Sharded** splits. Fusion was performed using 7000 data points sampled from the dataset seen by the first model. The same fusion data was used for last-layer KD as well. For the full table, please refer to Table 13.

METHOD	2-WAY SPLIT	4-WAY SPLIT	6-WAY SPLIT
Base Models	37.9, 36.6	19.4, 18.9, 18.7, 18.3	13.7, 13.3, 13.1 12.8, 12.4, 11.5
Vanilla Averaging	1.8 $\pm$ 0.4	1.2 $\pm$ 0.2	1.0 $\pm$ 0.0
Last-layer KD	36.0 $\pm$ 1.7	18.8 $\pm$ 2.3	12.8 $\pm$ 0.5
Ensemble	61.9 $\pm$ 0.6	50.2 $\pm$ 0.6	44.3 $\pm$ 0.5
<b>K-means Gradient Fusion (Ours)</b>	<b>49.4</b> $\pm$ 0.8	<b>38.5</b> $\pm$ 1.1	<b>33.1</b> $\pm$ 1.1

## 5.4 Full Dataset Setup

In their recent work, Solans et al. [2024] highlight that most fusion and aggregation algorithms are evaluated under a single training configuration, limiting insight into broader applicability. To this end, we also evaluate the performance of our algorithms on the setup where all models are trained on the full dataset but with different random seeds. Despite similar performance, these models occupy different regions in weight space, which presents an opportunity for a performance boost by fusion.

Table 3: **Test accuracy** comparison for ViTs trained and fine-tuned on CIFAR-100 in the **Full-Dataset** setup. Fusion used 6000 samples from the shared training dataset. We note that base models can slightly benefit from the fine-tuning phase as well; In 2-way fusion, the best accuracy ramped up to an average of 73.6, while for 4-way no model surpassed 74.2. Vanilla Averaging failed to retrain. For the full table, please refer to Table 14.

	Base Models	Zero-shot			Fine-tuning	
		Vanilla Averaging	K-means Gradient Fusion (Ours)	Ensemble	K-means Gradient Fusion (Ours)	Ensemble
2-way fusion:	73.4, 73.1	2.0 $\pm$ 0.1 -71.4	72.7 $\pm$ 0.1 -0.7	75.3 $\pm$ 0.1 +1.9	74.0 $\pm$ 0.3 +0.6	75.3 $\pm$ 0.0 +1.9
Inference Cost:	$\times$ 1	$\times$ 1	$\times$ 1	$\times$ 2	$\times$ 1	$\times$ 2
4-way fusion:	74.2, 73.6, 73.3, 73.7	1.3 $\pm$ 0.1 -72.9	71.8 $\pm$ 1.6 -2.5	76.7 $\pm$ 0.0 +2.5	74.5 $\pm$ 0.2 +0.3	76.9 $\pm$ 0.2 +2.7
Inference Cost:	$\times$ 1	$\times$ 1	$\times$ 1	$\times$ 4	$\times$ 1	$\times$ 4

While our algorithms were not specifically tailored to address this setup, we demonstrate in our experiments that we outperform baselines. Following prior work [Singh and Jaggi, 2020, Ainsworth et al., 2022], we evaluate our fusion algorithms by applying a *shared fine-tuning phase* to recover post-fusion performance. As in previous setups, we train VGGs on CIFAR-10 and ViTs on CIFAR-100, with three random seeds. Base models are sorted by pre-fusion accuracy and averaged. VGG11 results are in Table 10, and ViT in Table 3.

Fine-tuning is identical across all models: 200 epochs on the full dataset using a cosine learning rate schedule starting at  $10^{-5}$ . This differs from Imfeld et al. [2023], who perform a grid search over learning rates and epochs to select the best checkpoint. Although we intended to benchmark against Transformer OTFusion [Imfeld et al., 2023], we found the publicly available implementation difficult to adapt within our experimental timeline. Nevertheless, their fused models exhibit low zero-shot accuracy ( $< 12\%$ ), with the fine-tuning yielding modest gains ( $+0.8$ ), despite significantly weaker base model performance ( $< 65\%$  accuracy).

## 5.5 Fused Model Analysis and Insights

In this subsection we dive deeper into the clustering component of our algorithms, and we briefly explore the quality of fused models, in terms of robustness.

As shown in Appendix G, neuron importance scores consistently improve performance across fused models. Their main effect is during clustering, where they transform standard K-means into weighted K-means. Approximation is less sensitive to these scores (Appendix B.2). To illustrate this, we ablate on three MLPs (MNIST, non-IID, width 10) and compare clustering with uniform vs. Conductance-

based importance scores. Fig. 2 shows that weighting changes both cluster assignments and center positions.

In Fig. 3, we visualize the loss and accuracy landscapes of ViT base models trained on CIFAR-10, along with one of our fused models, using linear interpolation between model weights, as in Hochreiter and Schmidhuber [1997]. The contour plot reveals flatter basins around the fused model, which, as noted by Hochreiter and Schmidhuber [1997], is often indicative of improved generalization.

## 6 Limitations

Despite the strong performance of our proposed algorithms – often surpassing baselines and approaching that of ensembles – there remain areas for improvement.

First, the gradient-based variant of our approach is sensitive to hyperparameters and requires non-trivial tuning. While we were experimentally able to verify a set of hyperparameters that generalize well across our setups, this is not sufficient to claim universality.

Second, the effectiveness of our gradient-based fusion algorithm appears to scale with the size of the fusion dataset. While this dependency is encouraging in that more data yields better performance, it also highlights a shortcoming: the algorithm underperforms its linear counterpart when both are trained on the same limited data. This need can slow down the algorithm as demonstrated in Table 7.

## 7 Future Work

While our approach demonstrates strong empirical performance across a variety of fusion scenarios, several avenues remain open for further exploration and refinement.

**Automating Fusion Hyperparameter Selection and Level Partitioning.** Future work could explore principled methods for automatically tuning fusion hyperparameters, including the choice of level granularity and whether to end levels at before or after activation functions. In particular, task-specific heuristics could help adapt the level definitions for complex architectures like transformers.

**Beyond K-means for Grouping Optimization.** While this work uses Hungarian Matching and K-means Clustering to minimize grouping error, future research could evaluate more expressive or adaptive clustering methods to better capture inter-neuron similarity and improve fusion performance.

**Understanding the Contribution of Error Components.** A deeper investigation into the relative impact of grouping error versus approximation error on fusion quality could yield valuable insights.

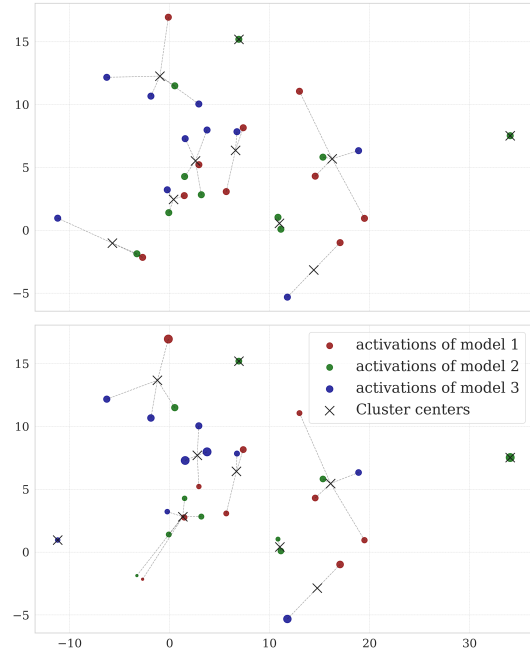


Figure 2: Clustering behavior with 3 MLPs on non-IID MNIST is shown under uniform (top) and conductance-based (bottom) importance scores. Marker sizes reflect neuron importance.

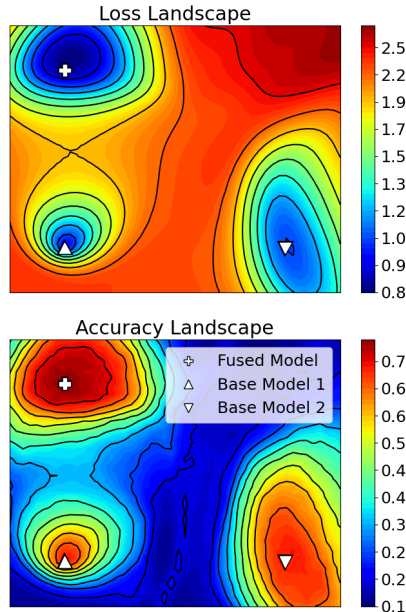


Figure 3: ViT Landscapes for CIFAR10, showing fused model from K-means Gradient Fusion using DeepLIFT scores

**Fusion as a Model Compression Technique.** Future work could explore using fusion to compress a large model into a smaller, more cost-efficient network. By leveraging the clustering process to distill representations, this paradigm may offer a new approach to model compression without retraining.

## 8 Conclusion

In this work, we introduced a novel neuron-aware approach to model fusion that supports fusing generic model architectures. Our algorithms, to our knowledge, are the first to successfully incorporate neuron importance scores in model fusion. Furthermore, our empirical results across diverse setups—including non-IID, sharded, and full-dataset regimes—consistently show that our fusion algorithms are competitive with or outperform existing baselines, especially in the zero-shot scenario, and in some cases approach ensemble-level performance.

## Acknowledgments

Andreas Spanopoulos gratefully acknowledges financial support from the *John S. Latsis Public Benefit Foundation*, the *Bodossaki Foundation*, and the *Union of Greek Shipowners*.

## References

- Samuel K Ainsworth, Jonathan Hayase, and Siddhartha Srinivasa. Git re-basin: Merging models modulo permutation symmetries. *arXiv preprint arXiv:2209.04836*, 2022.
- Daniel Aloise, Amit Deshpande, Pierre Hansen, and Preyas Popat. Np-hardness of euclidean sum-of-squares clustering. *Machine learning*, 75:245–248, 2009.
- Michael R. Berthold and Frank Höppner. On clustering time series using euclidean distance and pearson correlation. *CoRR*, abs/1601.02213, 2016. URL <http://arxiv.org/abs/1601.02213>.
- Leon Bottou and Yoshua Bengio. Convergence properties of the k-means algorithms. *Advances in neural information processing systems*, 7, 1994.
- Ekin D Cubuk, Barret Zoph, Dandelion Mane, Vijay Vasudevan, and Quoc V Le. Autoaugment: Learning augmentation policies from data. *arXiv preprint arXiv:1805.09501*, 2018.
- Kedar Dhamdhere, Mukund Sundararajan, and Qiqi Yan. How important is a neuron? *arXiv preprint arXiv:1805.12233*, 2018.
- Alexey Dosovitskiy, Lucas Beyer, Alexander Kolesnikov, Dirk Weissenborn, Xiaohua Zhai, Thomas Unterthiner, Mostafa Dehghani, Matthias Minderer, Georg Heigold, Sylvain Gelly, et al. An image is worth 16x16 words: Transformers for image recognition at scale. *arXiv preprint arXiv:2010.11929*, 2020.
- Shaimaa EK Ebid, Samah El-Tantawy, Doaa Shawky, and Hany L Abdel-Malek. Correlation-based pruning algorithm with weight compensation for feedforward neural networks. *Neural Computing and Applications*, pages 1–17, 2025.
- Leo Gao, Stella Biderman, Sid Black, Laurence Golding, Travis Hoppe, Charles Foster, Jason Phang, Horace He, Anish Thite, Noa Nabeshima, et al. The pile: An 800gb dataset of diverse text for language modeling. *arXiv preprint arXiv:2101.00027*, 2020.
- Geoffrey Hinton, Oriol Vinyals, and Jeff Dean. Distilling the knowledge in a neural network. *arXiv preprint arXiv:1503.02531*, 2015.
- Sepp Hochreiter and Jürgen Schmidhuber. Flat minima. *Neural computation*, 9(1):1–42, 1997.
- Moritz Imfeld, Jacopo Galdi, Marco Giordano, Thomas Hofmann, Sotiris Anagnostidis, and Sidak Pal Singh. Transformer fusion with optimal transport. *arXiv preprint arXiv:2310.05719*, 2023.
- Tapas Kanungo, David M Mount, Nathan S Netanyahu, Christine D Piatko, Ruth Silverman, and Angela Y Wu. A local search approximation algorithm for k-means clustering. In *Proceedings of the eighteenth annual symposium on Computational geometry*, pages 10–18, 2002.
- Diederik P Kingma and Jimmy Ba. Adam: A method for stochastic optimization. *arXiv preprint arXiv:1412.6980*, 2014.

- Narine Kokhlikyan, Vivek Miglani, Miguel Martin, Edward Wang, Bilal Alsallakh, Jonathan Reynolds, Alexander Melnikov, Natalia Kliushkina, Carlos Araya, Siqi Yan, and Orion Reblitz-Richardson. Captum: A unified and generic model interpretability library for pytorch, 2020. URL <https://arxiv.org/abs/2009.07896>.
- Harold W Kuhn. The hungarian method for the assignment problem. *Naval research logistics quarterly*, 2(1-2): 83–97, 1955.
- Alex Li, Yuandong Tian, Beidi Chen, Deepak Pathak, and Xinlei Chen. On the surprising effectiveness of attention transfer for vision transformers. *Advances in Neural Information Processing Systems*, 37:113963–113990, 2024.
- Stuart Lloyd. Least squares quantization in pcm. *IEEE transactions on information theory*, 28(2):129–137, 1982.
- Brendan McMahan, Eider Moore, Daniel Ramage, Seth Hampson, and Blaise Aguera y Arcas. Communication-efficient learning of deep networks from decentralized data. In *Artificial intelligence and statistics*, pages 1273–1282. PMLR, 2017.
- omihub777. Vit-cifar. <https://github.com/omihub777/ViT-CIFAR>. Accessed: 2025-05-16.
- Jaime Sevilla, Lennart Heim, Anson Ho, Tamay Besiroglu, Marius Hobbhahn, and Pablo Villalobos. Compute trends across three eras of machine learning. In *2022 International Joint Conference on Neural Networks (IJCNN)*, pages 1–8. IEEE, 2022.
- Avanti Shrikumar, Peyton Greenside, and Anshul Kundaje. Learning important features through propagating activation differences. In *International conference on machine learning*, pages 3145–3153. PMIR, 2017.
- Sidak Pal Singh and Martin Jaggi. Model fusion via optimal transport. *Advances in Neural Information Processing Systems*, 33:22045–22055, 2020.
- David Solans, Mikko Heikkilä, Andrea Vitaletti, Nicolas Kourtellis, Aris Anagnostopoulos, Ioannis Chatzigiannakis, et al. Non-iid data in federated learning: A survey with taxonomy, metrics, methods, frameworks and future directions. *arXiv preprint arXiv:2411.12377*, 2024.
- Mukund Sundararajan, Ankur Taly, and Qiqi Yan. Axiomatic attribution for deep networks. In *International conference on machine learning*, pages 3319–3328. PMLR, 2017.
- Ashish Vaswani, Noam Shazeer, Niki Parmar, Jakob Uszkoreit, Llion Jones, Aidan N Gomez, Łukasz Kaiser, and Illia Polosukhin. Attention is all you need. *Advances in neural information processing systems*, 30, 2017.
- Hongyi Wang, Mikhail Yurochkin, Yuekai Sun, Dimitris Papailiopoulos, and Yasaman Khazaeni. Federated learning with matched averaging. *arXiv preprint arXiv:2002.06440*, 2020.
- Yipei Xu, Dakuan Lu, Jiaqing Liang, Jin Zhao, Xintao Wang, Hengkui Wu, Ken Chen, Liujiang Liu, Yingsi Xin, Xuepeng Liu, et al. Source prompt: Coordinated pre-training of language models on diverse corpora from multiple sources. In *Proceedings of the 33rd ACM International Conference on Information and Knowledge Management*, pages 2732–2741, 2024.

## A Proofs

We first present the proof for Theorem 1.

*Proof.* We proceed to decompose the cost of Eq. (3) as follows, omitting the input  $\mathbf{x}$  for notational clarity:

$$\begin{aligned}
J_{\mathbf{w}^{\mathcal{F},i}}^{\text{IMP}} &= \sum_{j=1}^{d^i} s_j^i \min_k \left\{ \left( z_k^{\mathcal{F},i} - z_j^i \right)^2 \right\} \\
&= \sum_{j=1}^{d^i} s_j^i \left( z_{k_j}^{\mathcal{F},i} - z_j^i \right)^2 && \left( k_j \in \arg \min_k \left( z_k^{\mathcal{F},i} - z_j^i \right)^2 \right) \\
&= \sum_{j=1}^{d^i} s_j^i \left[ \left( z_{k_j}^{\mathcal{F},i} - T_{k_j} \right)^2 + 2 \left( z_{k_j}^{\mathcal{F},i} - T_{k_j} \right) \left( T_{k_j} - z_j^i \right) + \left( T_{k_j} - z_j^i \right)^2 \right] && \left( \pm T_{k_j} \right) \quad (6)
\end{aligned}$$

Since no constraints are imposed on the target vector  $\mathbf{T}$ , we retain the flexibility to define it in a manner that simplifies the optimization. Specifically, if we rearrange the summation in Eq. (6) into two nested summations – first over neurons in the fused model (i.e.,  $k = 1, \dots, l^{\mathcal{F},i}$ ), and then over original neurons  $j$  assigned to each  $k$  (i.e.,  $j : k_j = k$ ) – and define  $T_k$  as the importance-weighted mean of the assigned level outputs, i.e.,  $T_k = \frac{\sum_{j:k_j=k} s_j^i z_j^i}{\sum_{j:k_j=k} s_j^i}$ , then the cross-term in Eq. (6) vanishes:

$$\begin{aligned}
\sum_{j=1}^{d^i} 2s_j^i (z_{k_j}^{\mathcal{F},i} - T_{k_j}) (T_{k_j} - z_j^i) &= 2 \sum_{k=1}^{l^{\mathcal{F},i}} \sum_{j:k_j=k} s_j^i (z_k^{\mathcal{F},i} - T_k) (T_k - z_j^i) \\
&= 2 \sum_{k=1}^{l^{\mathcal{F},i}} (z_k^{\mathcal{F},i} - T_k) \sum_{j:k_j=k} s_j^i (T_k - z_j^i) \\
&= 2 \sum_{k=1}^{l^{\mathcal{F},i}} (z_k^{\mathcal{F},i} - T_k) \sum_{j:k_j=k} s_j^i \left( \frac{\sum_{l:k_l=k} s_l^i z_l^i}{\sum_{l:k_l=k} s_l^i} - z_j^i \right) \\
&= 2 \sum_{k=1}^{l^{\mathcal{F},i}} (z_k^{\mathcal{F},i} - T_k) \left( \sum_{l:k_l=k} s_l^i z_l^i - \sum_{j:k_j=k} s_j^i z_j^i \right) \\
&= 0
\end{aligned}$$

Therefore, Eq. (6) becomes:

$$\begin{aligned}
J_{\mathbf{w}^{\mathcal{F},i}}^{\text{IMP}} &= \sum_{j=1}^{d^i} s_j^i \left[ (z_{k_j}^{\mathcal{F},i} - T_{k_j})^2 + (T_{k_j} - z_j^i)^2 \right] \\
&= \sum_{k=1}^{l^{\mathcal{F},i}} \sum_{j:k_j=k} s_j^i \left[ (z_k^{\mathcal{F},i} - T_k)^2 + s_j^i (T_k - z_j^i)^2 \right] \quad (\text{re-express sum over output neurons})
\end{aligned}$$

□

We now present the proof for Theorem 2.

*Proof.* We analyze Hungarian Fusion and K-means Fusion separately.

**(a) Optimality of Hungarian Fusion:** As established in Section 4.1, the decoupled objective Eq. (4) separates into two terms: the *grouping error* and the *approximation error*. For linear levels, the layer outputs  $z_k^{\mathcal{F},i}$  are affine functions of the weights  $\mathbf{w}^{\mathcal{F},i}$ , and thus the approximation error reduces to a weighted least squares problem, which admits a closed-form solution.

Consequently, minimizing the total cost reduces to minimizing the grouping error. In the special case of two models with equal-sized layers and one-to-one neuron matching, this corresponds to a Linear Sum Assignment Problem (LSAP) with importance-weighted squared error as the cost matrix. The Hungarian algorithm solves this problem exactly in polynomial time [Kuhn, 1955], hence the HF algorithm returns the optimal solution.

**(b) Approximation Bound for K-means Fusion:** We consider a fixed assignment of neurons, where we assign the  $j^{\text{th}}$  base model neuron to the fused neuron  $k_j$ . Consider the total representation cost associated with all the base model neurons assigned to the  $k^{\text{th}}$  fused neuron for the layer  $i$  (in this proof we will omit the index  $i$  to simplify the notation). That is, the total representation cost of all base neurons  $j$  that have  $k_j = k$ . For a single sample, this is  $\sum_{j:k_j=k} s_j (z_k^{\mathcal{F}} - z_j)^2$ . If we stack this over the samples, we get  $\sum_{j:k_j=k} s_j \|\mathbf{z}_k^{\mathcal{F}} - \mathbf{z}_j\|^2$ , where  $\mathbf{z}_k^{\mathcal{F}}, \mathbf{z}_k \in \mathbb{R}^n$  are column vectors with each entry corresponding to the preactivation for one input sample. We let the previous layer's activations be  $\mathbf{X} \in \mathbb{R}^{n \times l^{\mathcal{F},i-1}}$ . Now, since it is a linear function of the previous layer's activations, we have  $\mathbf{z}_k^{\mathcal{F}} = \mathbf{X} \mathbf{w}_k$ , with  $\mathbf{w}_k$  being the weights associated with the  $k^{\text{th}}$  fused neuron (here we append a column of 1s to  $\mathbf{X}$  if we also have a bias term). Consider the projection matrix  $\mathbf{P} = \mathbf{X}(\mathbf{X}^T \mathbf{X})^+ \mathbf{X}^T$

that projects vectors to the column space of  $\mathbf{X}$ . Then  $\mathbf{I} - \mathbf{P}$  projects to the orthogonal complement of the image of  $\mathbf{X}$ . Recall that  $\mathbf{P}\mathbf{X} = \mathbf{X}$  and  $(\mathbf{I} - \mathbf{P})\mathbf{X} = 0$ . We then have

$$\begin{aligned}
\sum_{j:k_j=k} s_j \|\mathbf{z}_k^{\mathcal{F}} - \mathbf{z}_j\|^2 &= \sum_{j:k_j=k} s_j \|\mathbf{X}\mathbf{w}_k - \mathbf{z}_j\|^2 \\
&= \sum_{j:k_j=k} s_j \|\mathbf{P}(\mathbf{X}\mathbf{w}_k - \mathbf{z}_j) + (\mathbf{I} - \mathbf{P})(\mathbf{X}\mathbf{w}_k - \mathbf{z}_j)\|^2 \\
&= \sum_{j:k_j=k} s_j (\|\mathbf{P}(\mathbf{X}\mathbf{w}_k - \mathbf{z}_j)\|^2 + \|(\mathbf{I} - \mathbf{P})(\mathbf{X}\mathbf{w}_k - \mathbf{z}_j)\|^2) \\
&\hspace{15em} \text{(due to orthogonality)} \\
&= \sum_{j:k_j=k} s_j \|\mathbf{X}\mathbf{w}_k - \mathbf{P}\mathbf{z}_j\|^2 + \sum_{j:k_j=k} s_j \|(\mathbf{I} - \mathbf{P})\mathbf{z}_j\|^2
\end{aligned}$$

We consider the term  $\sum_{j:k_j=k} s_j \|\mathbf{X}\mathbf{w}_k - \mathbf{P}\mathbf{z}_j\|^2$ . Letting  $\bar{\mathbf{z}}_k = \frac{\sum_{j:k_j=k} s_j \mathbf{z}_j}{\sum_{j:k_j=k} s_j}$  (such that  $\sum_{j:k_j=k} s_j (\mathbf{P}\bar{\mathbf{z}}_k - \mathbf{P}\mathbf{z}_j) = 0$ ), we have

$$\begin{aligned}
\sum_{j:k_j=k} s_j \|\mathbf{X}\mathbf{w}_k - \mathbf{P}\mathbf{z}_j\|^2 &= \sum_{j:k_j=k} s_j \|(\mathbf{X}\mathbf{w}_k - \mathbf{P}\bar{\mathbf{z}}_k) + (\mathbf{P}\bar{\mathbf{z}}_k - \mathbf{P}\mathbf{z}_j)\|^2 \\
&= \sum_{j:k_j=k} s_j \|\mathbf{X}\mathbf{w}_k - \mathbf{P}\bar{\mathbf{z}}_k\|^2 + 2 \sum_{j:k_j=k} s_j (\mathbf{X}\mathbf{w}_k - \mathbf{P}\bar{\mathbf{z}}_k)^T (\mathbf{P}\bar{\mathbf{z}}_k - \mathbf{P}\mathbf{z}_j) \\
&\quad + \sum_{j:k_j=k} s_j \|\mathbf{P}\bar{\mathbf{z}}_k - \mathbf{P}\mathbf{z}_j\|^2 \\
&= \sum_{j:k_j=k} s_j \|\mathbf{X}\mathbf{w}_k - \mathbf{P}\bar{\mathbf{z}}_k\|^2 + 2(\mathbf{X}\mathbf{w}_k - \mathbf{P}\bar{\mathbf{z}}_k)^T \underbrace{\sum_{j:k_j=k} s_j (\mathbf{P}\bar{\mathbf{z}}_k - \mathbf{P}\mathbf{z}_j)}_{\rightarrow 0} \\
&\quad + \sum_{j:k_j=k} s_j \|\mathbf{P}\bar{\mathbf{z}}_k - \mathbf{P}\mathbf{z}_j\|^2 \\
&= \sum_{j:k_j=k} s_j \|\mathbf{X}\mathbf{w}_k - \mathbf{P}\bar{\mathbf{z}}_k\|^2 + \sum_{j:k_j=k} s_j \|\mathbf{P}\bar{\mathbf{z}}_k - \mathbf{P}\mathbf{z}_j\|^2
\end{aligned}$$

Thus, substituting this back, and summing over  $k$  to get the whole layer's representation cost, we get

$$\begin{aligned}
\sum_{k=1}^{l^{\mathcal{F}}} \sum_{j:k_j=k} s_j \|\mathbf{z}_k^{\mathcal{F}} - \mathbf{z}_j\|^2 &= \sum_{k=1}^{l^{\mathcal{F}}} \sum_{j:k_j=k} s_j \|\mathbf{X}\mathbf{w}_k - \mathbf{P}\bar{\mathbf{z}}_k\|^2 \\
&\quad + \sum_{k=1}^{l^{\mathcal{F}}} \sum_{j:k_j=k} s_j \|\mathbf{P}\bar{\mathbf{z}}_k - \mathbf{P}\mathbf{z}_j\|^2 + \sum_{j=1}^d s_j \|(\mathbf{I} - \mathbf{P})\mathbf{z}_j\|^2
\end{aligned}$$

Note first that the last term in the sum on the right is always incurred independently of the assignment  $k_j$  or the chosen weights  $\mathbf{w}_k$ .

Assume we have a solution that obtains the optimal representation cost  $OPT$ . Then, since the first term in the sum is nonnegative, the representative cost of the optimal solution is at least the optimal value of  $\sum_{k=1}^{l^{\mathcal{F}}} \sum_{j:k_j=k} s_j \|\mathbf{P}\bar{\mathbf{z}}_k - \mathbf{P}\mathbf{z}_j\|^2 + \sum_{j=1}^d s_j \|(\mathbf{I} - \mathbf{P})\mathbf{z}_j\|^2$ . If we let  $OPT_{grouping}$  be the minimum possible value of  $\sum_{k=1}^{l^{\mathcal{F}}} \sum_{j:k_j=k} s_j \|\mathbf{P}\bar{\mathbf{z}}_k - \mathbf{P}\mathbf{z}_j\|^2$ , then we get  $OPT \geq OPT_{grouping} + \sum_{j=1}^d s_j \|(\mathbf{I} - \mathbf{P})\mathbf{z}_j\|^2$

We now consider the sum on the right for KF. Recall that KF first projects the activations to the image of  $X$  and then finds the K-means clusters. That is, it finds the K-means clustering of  $(\mathbf{P}\mathbf{z}_j)_{j=1}^d$  to find the assignments  $k_j$ , aiming to minimize  $\sum_{k=1}^{l^{\mathcal{F}}} \sum_{j:k_j=k} s_j \|\mathbf{P}\bar{\mathbf{z}}_k - \mathbf{P}\mathbf{z}_j\|^2$ . Then, it fits  $\mathbf{w}_k$  such that  $\|\mathbf{X}\mathbf{w}_k - \mathbf{P}\bar{\mathbf{z}}_k\|^2$  is minimized by solving a weighted least squares problem as elaborated in Appendix B.2. Notice that this achieves  $\|\mathbf{X}\mathbf{w}_k - \mathbf{P}\bar{\mathbf{z}}_k\|^2 = 0$ , since, as  $\mathbf{P}\bar{\mathbf{z}}_k$  is in the image of  $\mathbf{X}$  by virtue of being a projection to that image, there is a  $\mathbf{w}_k$  satisfying  $\mathbf{X}\mathbf{w}_k = \mathbf{P}\bar{\mathbf{z}}_k$ . Thus, the total representation cost for KF for any layer will be  $\sum_{k=1}^{l^{\mathcal{F}}} \sum_{j:k_j=k} s_j \|\mathbf{P}\bar{\mathbf{z}}_k - \mathbf{P}\mathbf{z}_j\|^2 + \sum_{j=1}^d s_j \|(\mathbf{I} - \mathbf{P})\mathbf{z}_j\|^2$ , where the first term is the the weighted K-means loss with respect to clustering the projected preactivations, and the second term is always incurred regardless of assignment or chosen weights.

The K-means problem is NP-hard in general [Aloise et al., 2009]. However, the local-search algorithm introduced by Kanungo et al. [2002], provides a  $(9 + \epsilon)$ -approximation guarantee for the weighted K-means cost under squared Euclidean distance. By using this algorithm to construct the cluster assignments in KF, we obtain a solution where the term  $\sum_{k=1}^{l^{\mathcal{F}}} \sum_{j:k_j=k} s_j \|\mathbf{P}\bar{\mathbf{z}}_k - \mathbf{P}\mathbf{z}_j\|^2$  is within a constant factor of the optimal cost  $OPT_{grouping}$ .

Thus, the cost for this layer attained by KF is at most  $(9 + \epsilon)OPT_{grouping} + \sum_{j=1}^d s_j \|(\mathbf{I} - \mathbf{P})\mathbf{z}_j\|^2 \leq (9 + \epsilon)(OPT_{grouping} + \sum_{j=1}^d s_j \|(\mathbf{I} - \mathbf{P})\mathbf{z}_j\|^2) \leq (9 + \epsilon)OPT$ , showing that it is a  $(9 + \epsilon)$ -approximation for the layer representation cost.  $\square$

## B Efficiently Minimizing the Fusion Errors

### B.1 Minimizing the Grouping Error

For the special case (a), we can re-express Eq. (3) as a sum over the two base models:

$$J_{\mathbf{w}^{\mathcal{F},i}}^{\text{IMP}} = \sum_{j=1}^{d^{M_1,i}} s_j^{M_1,i} \min_k \left\{ \left( z_k^{\mathcal{F},i} - z_j^{M_1,i} \right)^2 \right\} + \sum_{j=1}^{d^{M_2,i}} s_j^{M_2,i} \min_k \left\{ \left( z_k^{\mathcal{F},i} - z_j^{M_2,i} \right)^2 \right\} \quad (7)$$

This cost can also be decomposed analogously to Eq. (4). We can now define the cost of matching neuron  $j_1$  of  $M_1$  to neuron  $j_2$  of  $M_2$ , as the cost of trying to approximate the resulting cluster center  $T_{j_1,j_2}$ , from any neuron of the fused model  $\mathcal{F}$ . A simpler alternative/heuristic is to just compute the distances between the level outputs. After defining this cost matrix, we can then run the Hungarian Matching algorithm [Kuhn, 1955] to find a one-to-one matching that minimizes Eq. (7).

For the general case (b), we can run Lloyd’s [Lloyd, 1982] algorithm for K-means, since it usually offers a good tradeoff between simplicity and effectiveness. By making use of the K-means++ initialization, we usually get better clusterings. Note that for this task, we treat neurons “as data points”, in the sense that we want to cluster neurons together. Therefore, the features of a neuron are the values (e.g. activations) it takes for different samples  $\mathbf{x}$  in the dataset. Clustering is then performed over these vectors using importance-weighted K-means, where the number of clusters “ $k$ ” is set to the desired number of neurons in the fused layer. Once clusters are formed, we compute the corresponding importance-weighted centroids, giving us the target matrix  $\mathbf{T} \in \mathbb{R}^{B \times l^{\mathcal{F},i}}$ , where  $B$  is the batch dimension.

### B.2 Minimizing the Approximation Error

For the special case where a level is a linear function of its weights  $\mathbf{w}^{\mathcal{F},i}$ , i.e.  $\mathbf{z}^{\mathcal{F},i} = \mathbf{X}\mathbf{w}^{\mathcal{F},i}$  for some  $\mathbf{X}$ , then the approximation error in Eq. (5) admits to a closed-form weighted-MSE solution:

$$\mathbf{w}^{\mathcal{F},i*} = (\mathbf{X}^\top \mathbf{S} \mathbf{X})^+ \mathbf{X}^\top \mathbf{S} \mathbf{T}^i$$

where  $\mathbf{S} = \text{diag}(s^i)$ , and  $()^+$  denotes the Moore-Penrose pseudoinverse.

For the general case, where a level is a non-linear differentiable function of its weights, we can obtain a local minima by optimizing with SGD. In practice we often use Adam [Kingma and Ba, 2014].

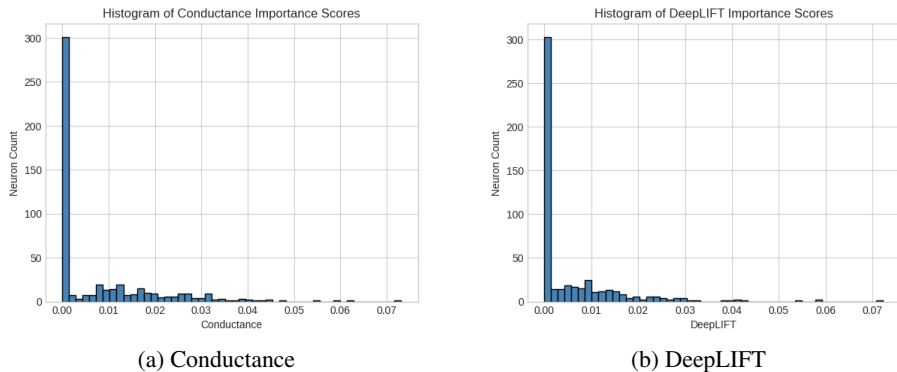


Figure 4: Histogram of Conductance and DeepLIFT Importance Scores

Furthermore, in practice, we do not minimize the weighted MSE, but rather the plain MSE. This is due to the fact that neurons with low importance scores will barely change if we use the weighted MSE. While this could only minimally affect the representation loss for the current level, it could lead to noisy inputs in later levels, or just poor intermediate representations. In our experiments we noticed that, especially in non-IID cases, many neurons tend to be attributed scores that are virtually zero as seen in Fig. 4.

## C Comparison of Hungarian Fusion with Existing Algorithms

We note that **Hungarian Fusion** is in spirit very similar to both **OTFusion** [Singh and Jaggi, 2020] and the activations-based version of **Git Re-Basin** [Ainsworth et al., 2022]. In the case of **Equal-size models with level-wise one-to-one matching** that we restrict HF to, they all construct a matching between neurons (or equivalent a transport map or permutation matrix to align the second model to the first) by solving a minimum cost matching problem.

However, a key difference is that HF accounts for the effect of refitting the previous layers and correspondingly refits the weights of the current layer being considered to minimize the effect of the accumulated error. Empirically, this significantly improves the zero-shot performance significantly as shown in our experimental results.

With regards to the incorporation of neuron importance scores, for OTFusion, Singh and Jaggi [2020] proposed using the neuron importance as the probability measure assigned to a neuron in the optimal transport problem setup, while Ainsworth et al. [2022] did not discuss applying importance scores in Git Re-Basin. In our experiments, we follow the recommendation of Singh and Jaggi [2020] for OTFusion and for Git Re-Basin we weigh the neuron weights according to the neuron’s score when averaging, in the same manner as we do for HF.

## D Data Partitioning Regimes

### D.1 Non-IID Splits

To simulate non-IID splits, we utilize a Dirichlet distribution to create unbalanced class distributions across models. Let  $N_c$  represent the number of data points in class  $c$ , and  $\alpha_k$  denote the concentration parameter for model  $k$ . The data for each class  $c$  is distributed across models as:

$$\text{split}_k \sim \text{Dir}(\alpha_1, \dots, \alpha_k)$$

where  $\text{Dir}(\cdot)$  represents the Dirichlet distribution. The concentration parameters  $\alpha_k$  are arranged in an ordered sequence, determined by the parameter `min_max_ratio`:

```
alpha_min = 1.0
min_max_ratio = 0.2
alpha_max = alpha_min / min_max_ratio
```

```
alphas = linspace(alpha_min, alpha_max, min_max_ratio)
```

A smaller ratio results in a wider disparity between splits, amplifying the heterogeneity. The Dirichlet-distributed probabilities dictate the number of samples assigned to each model for class  $c$ , ensuring that splits exhibit diverse and non-uniform class distributions. Random shuffling of *class indices* and *concentration parameters* for each class  $c$  introduces additional randomness in the resulting splits.

## D.2 Sharded Splits

In the sharded partitioning regime, the dataset is split such that each model receives examples from a disjoint subset of classes. That is, no two models share any classes in their local datasets, simulating a strongly divergently distributed base model training datasets scenario based on class exclusivity rather than distributional imbalance.

Let  $\mathcal{C}$  denote the set of all classes in the dataset. The class set is first randomly permuted and then evenly partitioned into  $K$  disjoint subsets, where  $K$  is the number of models. Each subset  $\mathcal{C}_k$  is assigned to model  $k$ , and all examples belonging to classes in  $\mathcal{C}_k$  are included in that model’s local dataset:

$$\bigcup_{k=1}^K \mathcal{C}_k = \mathcal{C}, \quad \mathcal{C}_i \cap \mathcal{C}_j = \emptyset \quad \forall i \neq j$$

## E Model Training Details

We trained **VGGs on CIFAR-10** and **ViTs on CIFAR100**. All models were trained on NVIDIA RTX A5000 GPUs.

The VGGs followed the VGG11 architecture and the implementation is based on the open source implementation provided by <sup>2</sup>Singh and Jaggi [2020].

The ViTs implementation is based on <sup>3</sup>omihub777, and we used the following model hyperparameters:

Model Hyperparameter	Value
Patch Size	8
Attention Heads	12
Encoder Blocks	7
Feed Forward Network Hidden Size	384
Encoder Hidden Size	384

To train the models, we use the non-exhaustive list of hyperparameters listed in Table 4

Splits	VGG Epochs	ViT Epochs	Training Hyperparameter	Value
Full Dataset	300	350	Warmup Epochs	5
Split By 2	200	250	Minimum Learning Rate	$10^{-5}$
Split By 4	150	225	Learning Rate	$10^{-3}$
Split By 6	–	200	Label Smoothing	0.1
Split By 8	125	–	Batch Size	128

(a) Number of training epochs

(b) Training hyperparameters

Table 4: Training configurations and schedules for VGG and ViT models.

The following torch augmentations were used for training: RandomCrop, RandomHorizontalFlip, Normalize, and other augmentations as in omihub777 based on Cubuk et al. [2018].

The model was trained using torch’s Gradual Warmup Scheduler with torch’s CosineAnnealingLR scheduler.

<sup>2</sup><https://github.com/sidak/otfusion>

<sup>3</sup><https://github.com/omihub777/ViT-CIFAR>

We believe that these are sufficient to reproduce the main claims of our work. Additional information about hyperparameters can be found in our open-source code repository.

## F Fusion Implementation Details

### F.1 Fusion Hyperparameters

Our proposed fusion algorithms include both linear and gradient-based variants, each with distinct hyperparameter considerations.

**Linear Variants.** The linear fusion algorithms (e.g., plain Hungarian Fusion and K-means Fusion) require minimal hyperparameter tuning. The primary decisions involve whether to normalize (i) neuron outputs and/or (ii) neuron importance scores. In our experiments, we found that omitting normalization typically yielded better results across both all data partitioning settings. This is likely because normalization can distort relative differences in neuron output magnitude that are informative for matching or clustering.

**Gradient-based Variants.** In contrast, the gradient-based fusion variant introduces a broader set of hyperparameters. These include:

1. **Optimization Parameters:** learning rate, weight decay, number of gradient steps per level, and batch size, validation split, validation patience.
2. **Initialization Scheme:** initialization of the fused model weights at each level (e.g., weights from a randomly selected base model with added noise  $\epsilon$ ).
3. **Clustering Settings:** number of clusters (typically matched to the fused model’s layer width), use of K-means++ initialization, early stopping criteria and whether to normalize neuron outputs just for the clustering stage.
4. **Importance Weighting:** whether and how to incorporate neuron importance scores into both clustering and loss weighting.

While this added complexity increases flexibility and modeling capacity, it also requires careful tuning for stable and effective optimization. To mitigate this, we conducted extensive experiments and identified two sets of hyperparameter configurations that generalized well across datasets (CIFAR-10, CIFAR-100), model architectures (VGG11, ViT), and fusion regimes (Full Dataset, Non-IID, Sharded). Specifically, we found the hyperparameters in Table 5.

Table 5: Sets of hyperparameters used for K-means Gradient Fusion

Hyperparameter	Setting 1	Setting 2
Optimizer ( $n - 1$ first levels)	Adam	SGD
Learning Rate ( $n - 1$ first levels)	$10^{-3}$	$10^{-4}$
Epochs ( $n - 1$ first levels)	100	50
Weight Decay (All levels)	$10^{-4}$	$10^{-4}$
Perturbation $\epsilon$	1.0	0.1
Optimizer (Last level)	Adam	Adam
Learning Rate (Last level)	$10^{-3}$	$10^{-3}$
Epochs (Last level)	100	100
Epochs ( $n - 1$ first levels)	100	100
Normalize Activations	False	False
Train Batch Size	32	32
Val Split	0.1	0.1
Head Weights	True	True

We note that “Head Weights” refers to weighing the final logits of the models by the proportion of samples seen per class, for every model. In practice, this heuristic improves accuracy by a small margin, but this comes at a cost of calibration, as the test loss increases.

Each setting of hyperparameters induces a different behavior in the gradient-based variant of our algorithm. By using Setting 1, we essentially take larger gradient steps that move us far away from initialization. The resulting model is quite different from base models, in terms of plain weight L2 norm. On the other hand, Setting 2 relies on the initialization of the model to be already decent (e.g. any base model), and takes small gradient steps. Empirically, we found that with the second setting, the majority of performance gain occurs at the classification head, where the targets become the raw average logits of all base models. This is similar to Knowledge Distillation (KD), with the only difference that KD typically minimizes some sort of KL-divergence loss between softmaxed logits and average-softmaxed base-model-logits, instead of minimizing the L2 distance between averaged raw logits. Nevertheless, the interesting models are produced with the first setting, which finds new solutions far away from initialization, and within a much richer context.

For our experiments:

- **All** Full-dataset models were fused using *Setting 1*.
- **All** sharded models were fused using *Setting 1*.
- **All** Non-IID models, **except** for VGG11s and ViTs with  $n = 2$  models for CIFAR-10 (which used Setting 1), were fused using *Setting 2*.

While training full-dataset models, we used setting 1, but also normalized activations for k-means. In our experiments, we observed that this did not yield significant improvements.

## F.2 Model Partitioning Schemes

Due to the flexibility of our algorithm, we had the freedom to develop our own partition. In practice we as we primarily tested on like models, there were obvious answers that we used.

For VGG11s, each level contained only a single convolutional or linear layer to be aligned or an activation function, which did not need to be aligned.

For ViTs, each level corresponded to an encoder block except for the last one which corresponded to the classifier head.

## F.3 Post Fusion Finetuning Hyperparameters

For fusing full dataset models, a finetuning phase is shown to improve fused model performance above base model performance. For this finetuning phase we used torch’s CosineAnnealingWarmRestarts scheduler. The whole process had the following hyperparameters:

Hyperparameter	Value
Learning Rate	$10^{-4}$
Minimum Learning Rate	$10^{-6}$
Label Smoothing	0.1
Epochs	200

The augmentation was the same generic suite as we used to train VGGs and ViTs initially. See Appendix E for more details. Once again, all code for reproduction is present in our open source repository.

## F.4 Neuron Importance Score Implementation

We heavily rely on [Kokhlikyan et al. \[2020\]](#) to compute importance scores for us. We built a framework around it that batches our requests, but the package does the lion’s share of the work in computing both Conductance [\[Dhamdhere et al., 2018\]](#) and DeepLIFT [Shrikumar et al. \[2017\]](#).

## F.5 Algorithm Runtime Comparison

As our methods are technically specific implementations of our general framework, it is difficult to definitively give an evaluation of the overall framework. However, we did quantify the performance

of our realizations, both on VGGs and ViTs. We only used importance scores for VGGs as they just add a constant startup time and usually do not interfere with the performance of the algorithm. For the same reason, we only use conductance when testing for importance score times. Interestingly, KF Linear speeds up significantly when we use importance scores, suggesting that the K-means portion of the algorithm resolves faster in this case because of the weights. All experiments were ran on NVIDIA RTX A5000 GPUs.

Table 6: **Algorithm runtime** comparison when fusing VGG networks on CIFAR-10. We fused the same two models 10 times and averaged the run times. All algorithms were run with the same 400 samples in each iteration. All times are in seconds.

Algorithm	Runtime (Uniform)	Runtime (Conductance)
OT Fusion	0.7	3.0
Git Re-Basin	1.0	3.2
HF Linear (Ours)	14.2	16.5
KF Linear (Ours)	78.3	83.7
KF Gradient Uniform (Ours)	16.5	18.8

Table 7: **Algorithm runtime** comparison when fusing ViT networks on CIFAR-100. We fused the same two models 5 times using our KF Gradient method with uniform importance scores and averaged the run times.

Fusion Samples	Runtime (s)
400	38.1
6000	632.5

## G Additional Results

In this section, besides complimentary tables, we will also present the full tables for results shown earlier. These full tables include the standard deviation for base models, as well as the performance of each fusion algorithm for each neuron importance score.

Table 8: **Test accuracy** comparison when fusing ViT networks on CIFAR-100 for **Non-IID** splits. Fusion used 7000 samples from the dataset seen by the first model. The same fusion data was used for last-layer KD as well. For the full table, refer to Table 12.

Method	2-WAY SPLIT	4-WAY SPLIT	6-WAY SPLIT
Base Models	54.5, 50.9	48.4, 46.3, 45.0, 43.5	41.3, 40.5, 40.1 38.7, 37.7, 28.8
Vanilla Averaging	1.6 $\pm$ 0.3	1.0 $\pm$ 0.3	1.2 $\pm$ 0.6
Last-layer KD	51.0 $\pm$ 1.4	43.0 $\pm$ 1.1	35.7 $\pm$ 1.6
Ensemble	66.7 $\pm$ 0.1	60.8 $\pm$ 0.8	53.8 $\pm$ 1.2
K-means Gradient Fusion (Ours)	<b>57.1</b> $\pm$ 0.9	<b>51.7</b> $\pm$ 1.2	<b>45.1</b> $\pm$ 0.9

Table 9: **Test accuracy** comparison when fusing VGG11 networks on CIFAR-10 for **Sharded** splits. Fusion was performed using 400 data points sampled from the dataset seen by the first model. The same fusion data was used for all algorithms.

METHOD	2-WAY SPLIT	4-WAY SPLIT	6-WAY SPLIT
Individual Models	47.16, 46.59	28.93, 28.46 19.37, 16.54	19.88, 19.70, 19.34 16.63, 10.00, 10.00
Vanilla Averaging	12.36 $\pm$ 2.6	10.00 $\pm$ 0.0	10.00 $\pm$ 0.0
Last-layer KD	50.60 $\pm$ 1.5	32.08 $\pm$ 1.3	22.00 $\pm$ 1.0
Ensemble	79.22 $\pm$ 1.7	53.50 $\pm$ 2.7	41.52 $\pm$ 3.2
OTFusion	24.81 $\pm$ 3.5	11.20 $\pm$ 2.6	10.00 $\pm$ 0.0
Git Re-Basin	55.65 $\pm$ 5.1	N/A	N/A
Hungarian Linear Fusion (Ours)	73.16 $\pm$ 4.1	N/A	N/A
K-means Linear Fusion (Ours)	73.44 $\pm$ 4.4	43.91 $\pm$ 3.4	<b>33.73</b> $\pm$ 2.9
K-means Gradient Fusion (Ours)	<b>76.06</b> $\pm$ 1.7	<b>43.97</b> $\pm$ 2.4	31.95 $\pm$ 3.6

Table 10: **Test accuracy** comparison for VGGs trained and fine-tuned on CIFAR-10 in the **Full-Dataset** setup. Fusion used 400 samples from the shared training dataset. We note that base models can benefit from the fine-tuning phase as well, but the gain is marginal; In 2-way fusion, the best accuracy ramped up to an average of 91.6. Full results can be accessed in Table 15.

	Base Models	Zero-shot		Fine-tuning	
		K-means Gradient Fusion (Ours)	Ensemble	K-means Gradient Fusion (Ours)	Ensemble
2-way:	91.2, 91.0	91.0 $\pm$ 0.0	92.1 $\pm$ 0.1	91.7 $\pm$ 0.0	92.1 $\pm$ 0.1
Efficiency:	$\times 2$	$\times 2$	$\times 1$	$\times 2$	$\times 1$

Table 11: **Test accuracy** comparison when fusing VGG11 networks on CIFAR-10 for **Non-IID** splits. This table is complimentary to Table 1.

Method	2-WAY SPLIT	4-WAY SPLIT	8-WAY SPLIT
Individual Models	81.5 $\pm$ 1.9, 75.1 $\pm$ 2.4	77.2 $\pm$ 3.7, 75.3 $\pm$ 3.3, 73.6 $\pm$ 2.3, 66.8 $\pm$ 3.7	69.2 $\pm$ 2.4, 68.0 $\pm$ 1.4, 66.0 $\pm$ 1.2, 63.0 $\pm$ 2.3 61.8 $\pm$ 2.4, 59.6 $\pm$ 1.5, 56.1 $\pm$ 3.3, 52.6 $\pm$ 4.8
Vanilla Averaging	11.2 $\pm$ 2.2	10.0 $\pm$ 0.0	10.0 $\pm$ 0.0
Last-layer KD	82.7 $\pm$ 0.9	60.1 $\pm$ 6.8	43.7 $\pm$ 9.8
Ensemble	87.5 $\pm$ 0.4	83.7 $\pm$ 0.9	76.6 $\pm$ 0.7
OTF Uniform	43.4 $\pm$ 6.9	20.4 $\pm$ 7.6	12.9 $\pm$ 2.6
OTF Conductance	42.6 $\pm$ 4.0	13.9 $\pm$ 3.4	13.7 $\pm$ 3.0
OTF DeepLIFT	39.8 $\pm$ 7.8	14.0 $\pm$ 3.5	14.0 $\pm$ 3.1
Git Re-Basin Uniform	53.8 $\pm$ 6.2	N/A	N/A
Git Re-Basin Conductance	69.7 $\pm$ 6.7	N/A	N/A
Git Re-Basin DeepLIFT	71.8 $\pm$ 3.4	N/A	N/A
HF Linear Uniform (Ours)	72.3 $\pm$ 0.6	N/A	N/A
HF Linear Conductance (Ours)	84.6 $\pm$ 0.7	N/A	N/A
HF Linear DeepLIFT (Ours)	<b>84.6</b> $\pm$ 0.8	N/A	N/A
KF Linear Uniform (Ours)	83.5 $\pm$ 1.1	77.8 $\pm$ 1.0	67.6 $\pm$ 0.9
KF Linear Conductance (Ours)	84.5 $\pm$ 0.8	<b>78.9</b> $\pm$ 1.3	<b>69.6</b> $\pm$ 1.2
KF Linear DeepLIFT (Ours)	84.3 $\pm$ 0.8	78.8 $\pm$ 1.3	69.3 $\pm$ 0.8
KF Gradient Uniform (Ours)	83.2 $\pm$ 1.2	78.5 $\pm$ 2.1	68.4 $\pm$ 4.9
KF Gradient Conductance (Ours)	83.3 $\pm$ 1.1	78.6 $\pm$ 2.1	68.6 $\pm$ 4.5
KF Gradient DeepLIFT (Ours)	83.3 $\pm$ 1.1	78.6 $\pm$ 2.1	68.4 $\pm$ 4.8

Table 12: **Test accuracy** comparison when fusing ViT networks on CIFAR-100 for **Non-IID** splits. This table is complimentary to Table 8.

Method	2-WAY SPLIT	4-WAY SPLIT		6-WAY SPLIT		
Individual Models	54.5 $\pm$ 0.7	48.4 $\pm$ 0.9	46.3 $\pm$ 0.5	41.3 $\pm$ 1.0,	40.5 $\pm$ 0.9,	40.1 $\pm$ 0.6
	50.9 $\pm$ 2.8	45.0 $\pm$ 0.7	43.5 $\pm$ 1.7	38.7 $\pm$ 1.0	37.7 $\pm$ 2.1	28.8 $\pm$ 7.9
Vanilla Averaging	1.6 $\pm$ 0.3	1.0 $\pm$ 0.3		1.2 $\pm$ 0.6		
Last-layer KD	51.0 $\pm$ 1.4	43.0 $\pm$ 1.1		35.7 $\pm$ 1.6		
Ensemble	66.7 $\pm$ 0.1	60.8 $\pm$ 0.8		53.8 $\pm$ 1.2		
KF Gradient Uniform (Ours)	57.0 $\pm$ 1.0	51.7 $\pm$ 1.4		45.1 $\pm$ 0.9		
KF Gradient Conductance (Ours)	57.0 $\pm$ 0.9	51.7 $\pm$ 1.2		44.9 $\pm$ 0.8		
KF Gradient DeepLIFT (Ours)	57.1 $\pm$ 0.9	51.7 $\pm$ 1.3		44.9 $\pm$ 0.8		

Table 13: **Test accuracy** comparison when fusing ViT networks on CIFAR-100 for **Sharded** splits. This table is complimentary to Table 2.

Method	2-WAY SPLIT	4-WAY SPLIT		6-WAY SPLIT		
Individual Models	37.9 $\pm$ 0.3	19.4 $\pm$ 0.4	18.9 $\pm$ 0.2	13.7 $\pm$ 0.3,	13.3 $\pm$ 0.2	13.1 $\pm$ 0.2
	36.6 $\pm$ 0.4	18.7 $\pm$ 0.1	18.3 $\pm$ 0.4	12.8 $\pm$ 0.2	12.4 $\pm$ 0.4	11.5 $\pm$ 0.5
Vanilla Averaging	1.8 $\pm$ 0.4	1.2 $\pm$ 0.2		1.0 $\pm$ 0.0		
Last-layer KD	36.0 $\pm$ 1.7	18.8 $\pm$ 2.3		12.8 $\pm$ 0.5		
Ensemble	61.9 $\pm$ 0.6	50.2 $\pm$ 0.6		44.3 $\pm$ 0.5		
KF Gradient Uniform (Ours)	46.9 $\pm$ 0.9	37.1 $\pm$ 1.4		31.6 $\pm$ 0.5		
KF Gradient Conductance (Ours)	49.3 $\pm$ 0.9	38.1 $\pm$ 1.3		33.1 $\pm$ 1.1		
KF Gradient DeepLIFT (Ours)	49.4 $\pm$ 0.8	38.5 $\pm$ 1.1		33.0 $\pm$ 0.5		

Table 14: **Test accuracy** comparison when fusing ViT networks on CIFAR-100 trained on the full dataset. This table is complimentary to Table 3.

Method	2-WAY ZERO-SHOT	2-WAY FINETUNED	4-WAY ZERO-SHOT	4-WAY FINETUNED
Individual Models	73.4 $\pm$ 0.1	73.6 $\pm$ 0.3	74.2 $\pm$ 0.2, 73.6 $\pm$ 0.2,	74.2 $\pm$ 0.1, 73.8 $\pm$ 0.1,
	73.1 $\pm$ 0.1	73.1 $\pm$ 0.1	73.3 $\pm$ 0.1, 73.0 $\pm$ 0.0	73.3 $\pm$ 0.3, 73.0 $\pm$ 0.0
Vanilla Averaging	2.0 $\pm$ 0.1	1.9 $\pm$ 0.1	1.3 $\pm$ 0.1	1.5 $\pm$ 0.5
Ensemble	75.2 $\pm$ 0.1	75.3 $\pm$ 0.0	76.6 $\pm$ 0.0	76.9 $\pm$ 0.2
KF Gradient Uniform (Ours)	72.7 $\pm$ 0.4	73.9 $\pm$ 0.3	71.8 $\pm$ 1.6	74.5 $\pm$ 0.2
KF Gradient Conductance (Ours)	72.6 $\pm$ 0.4	73.9 $\pm$ 0.4	71.1 $\pm$ 2.3	74.3 $\pm$ 0.0
KF Gradient DeepLIFT (Ours)	72.6 $\pm$ 0.3	74.0 $\pm$ 0.3	71.6 $\pm$ 1.7	74.4 $\pm$ 0.1

Table 15: **Test accuracy** comparison when fusing VGG11 networks pairwise on CIFAR-10 trained on the full dataset. Results are averages across seeds. Fusion was performed using 400 data points sampled from the dataset. The same fusion data was used for all algorithms. This table is complimentary to Table 10.

Method	ZERO-SHOT	FINETUNED
Individual Models	91.2 $\pm$ 0.0	91.6 $\pm$ 0.0
	90.1 $\pm$ 0.2	91.5 $\pm$ 0.1
Vanilla Averaging Ensemble	12.2 $\pm$ 1.8	12.5 $\pm$ 1.9
	92.1 $\pm$ 0.1	92.4 $\pm$ 0.1
OTF Uniform	75.2 $\pm$ 2.6	91.3 $\pm$ 0.1
OTF Conductance	65.5 $\pm$ 2.0	91.6 $\pm$ 0.1
OTF DeepLIFT	66.8 $\pm$ 1.3	91.5 $\pm$ 0.2
Git Re-Basin Uniform	75.7 $\pm$ 1.4	91.3 $\pm$ 0.1
Git Re-Basin Conductance	77.0 $\pm$ 0.8	92.7 $\pm$ 0.1
Git Re-Basin DeepLIFT	75.7 $\pm$ 1.4	<b>92.8</b> $\pm$ 0.1
HF Linear Uniform (Ours)	84.1 $\pm$ 0.2	90.8 $\pm$ 0.0
HF Linear Conductance (Ours)	90.8 $\pm$ 0.0	92.7 $\pm$ 0.1
HF Linear DeepLIFT (Ours)	90.8 $\pm$ 0.1	92.6 $\pm$ 0.1
KF Linear Uniform (Ours)	90.5 $\pm$ 0.2	92.5 $\pm$ 0.2
KF Linear Conductance (Ours)	90.4 $\pm$ 0.1	92.6 $\pm$ 0.1
KF Linear DeepLIFT (Ours)	90.5 $\pm$ 0.2	92.6 $\pm$ 0.2
KF Gradient Uniform (Ours)	<b>91.0</b> $\pm$ 0.0	91.7 $\pm$ 0.0
KF Gradient Conductance (Ours)	<b>91.0</b> $\pm$ 0.1	91.7 $\pm$ 0.1
KF Gradient DeepLIFT (Ours)	<b>91.0</b> $\pm$ 0.1	91.6 $\pm$ 0.0

## H Existing Assets and Licenses

We make use of code from the following sources:

1. OTFusion [Singh and Jaggi \[2020\]](#), Open Source, <https://github.com/sidak/otfusion>.
2. ViT-CIFAR [omihub777](#), MIT License, <https://github.com/omihub777/ViT-CIFAR/blob/main/LICENSE>.
3. Captum [Kokhlikyan et al. \[2020\]](#), BSD 3-Clause License, <https://github.com/pytorch/captum/blob/master/LICENSE>.

## I Broader Impact

This work concerns foundational research on model fusion algorithms. We do not foresee any negative applications beyond those broadly applicable to model fusion algorithms.

As with other fusion methods, negative societal impacts may follow from using biased or harmful models as a base model to perform fusion as the fused model may contain the biases / harmful potential of the base model.